

Electronic Supplementary Information

Cost-effective Large-scale Synthesis of ZnO Photocatalyst with Excellent Performance for dye photodegradation

Chungui Tian, Qi Zhang, Aiping Wu, Meijia Jiang, Zhengliang Liang, Baojiang Jiang and Honggang Fu

1. Experimental section

Zn(Ac)₂•2H₂O was purchased from Tianjing Kermel Chemical Reagent Co., Ltd., and was used as received without further purification.

The preparation of ZnO is very simple. The evaporating dish with 28g of Zn(Ac)₂•2H₂O solid was placed into a muffle furnace, for which the temperature was increased from room temperature to 600 degree with a heating rate of 5 ° min⁻¹ in an air atmosphere and kept at the maximum temperature for 120 min. After naturally cooling to room temperature, the white powder was collected. The sample was denoted as ZnO-600, where 600 refer to the temperature. The quality of ZnO is about 9.9g, corresponding to the higher yield of 97%. **Both the production and yield of this solid phase route are much higher than that of solution-based methods.** To study the effect of temperature on the microstructure and performance, ZnO-400, ZnO-800 and ZnO-900 catalysts were also prepared.

2. Characterization

Transmission electron microscopy (TEM, JEOL-2010) with an acceleration voltage of 200 kV was used to characterize the morphology of samples. X-ray powder diffraction (XRD) was performed with a Rigaku (Japan) D/MAX-rA X-ray diffractionmeter equipped with graphite monochromatized Cu K α radiation ($\gamma=1.541874 \text{ \AA}$). Fourier transform infrared (FT-IR) spectra were carried out on NICOLETiS10 FT-IR spectrometer. X-ray photoemission spectroscopy (XPS) studies were carried out on a Kratos-AXIS UL TRA DLD with Al K α radiation source. The nitrogen adsorption/desorption isotherms were measured at 77 K using a

Micromeritics Tristar[□]. Before measurement, the samples were out gassed at 150 □ for 4.5 h; the specific surface area of the materials was calculated by the Brunauer–Emmett–Teller (BET) theory.

3. Photocatalytic test

The photocatalytic performance of ZnO was evaluated by using Methyl Orange (MO), Rhodamine B (RhB) and Methylene Blue (MB) dye as representative pollutants. In detail, 0.05 g catalyst (ZnO, Degussa P25) and 40 mL of 10mg/L dye (MO, RhB and MB) aqueous solution was mixed in a 100 mL reaction cylinder under ultrasound. After stirring in the dark for 30 min to reach the adsorption equilibrium, the suspension was irradiated with 15-W UV light-tube (365 nm) for a given time under continuous magnetic stirring. A UV-2550 spectrometer was used to measure the concentration of dye molecules. The parameters in recycled experiments are the same as those in the first testing, excepting that the catalyst was recollected by centrifugation at 3500 rpm/min (for ZnO) and 8000 rpm/min (for P25 TiO₂).

4. The photography of ZnO-600 sample

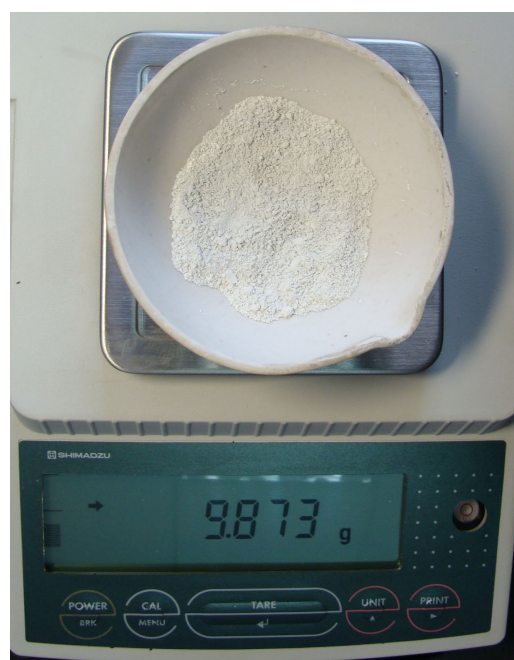


Fig. S1 The photography of ZnO prepared by calcination of Zinc acetate at 600 °C. For one time preparation, about 9.9g of ZnO could be obtained by calcination of 28g of Zinc acetate, corresponding to the high yield of 97%. The deviation of experimental value from the theoretically calculated value should be due to the residue of products on the Evaporating dish. Also, the synthesis could be easily scaled-up due to the solid-based reaction process.

5. XRD and IR characterization

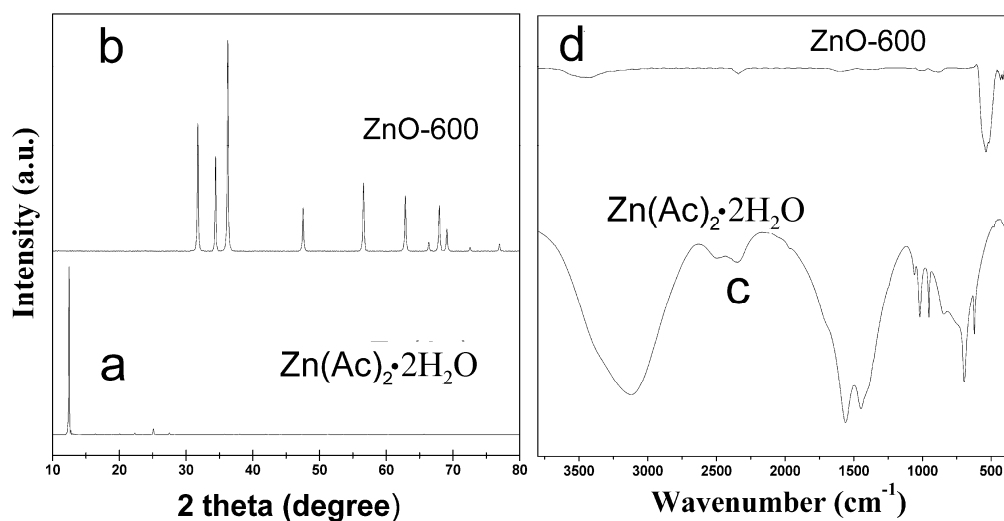


Fig. S2 XRD patterns and IR spectra of $\text{Zn}(\text{Ac})_2 \cdot 2\text{H}_2\text{O}$ and ZnO-600 .

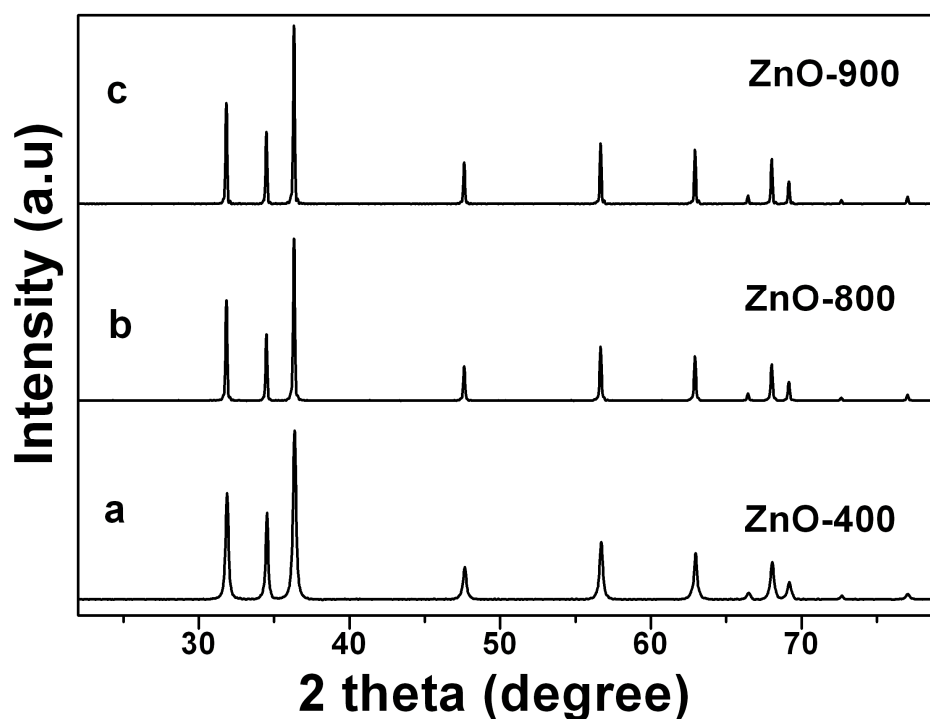


Fig. S3 XRD patterns of (a) ZnO-400 , (b) ZnO-800 and (c) ZnO-900 . All peaks in these patterns can be indexed to the diffractions of hexagonal (wurtzite) structure ZnO .

6. TEM images

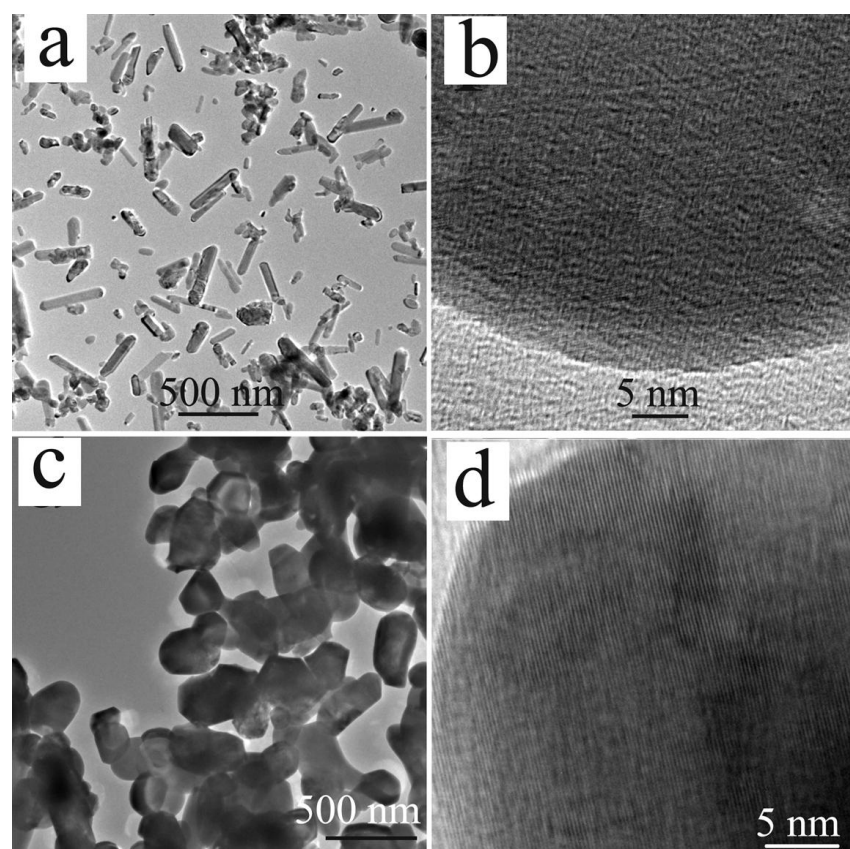


Fig. S4 TEM and HRTEM images of (a,b) ZnO-400 and (c,d) ZnO-800.

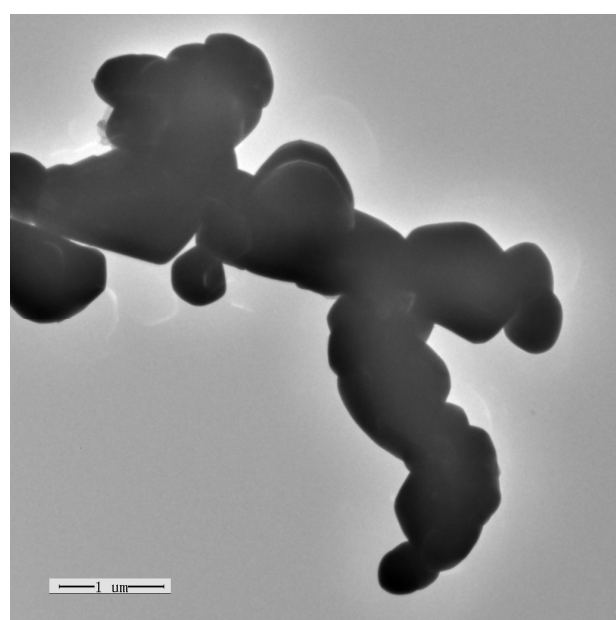


Fig. S5 TEM image of ZnO-900.

7. Photocatalytic activity for the photodecomposition of MO

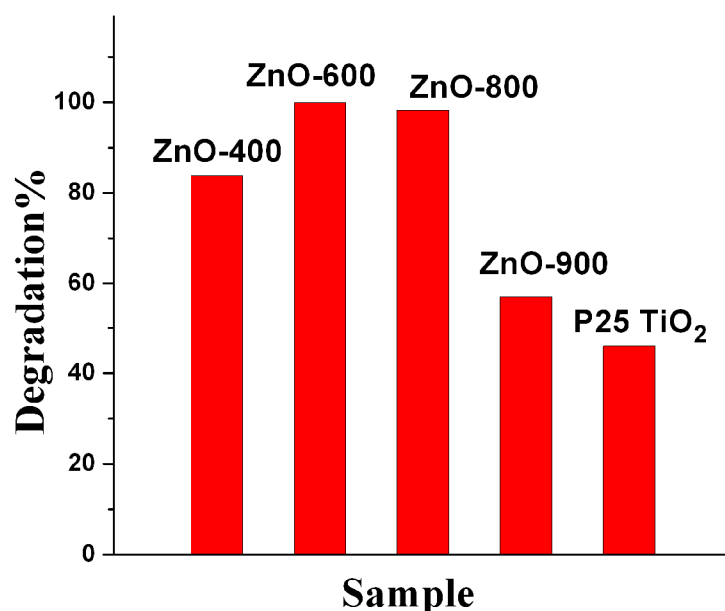


Fig. S6 The catalytic activity of ZnO samples and P25 for photodegradation of MO.

8. Stability

After photocatalytic reaction, the solids were separated and then characterized by XRD and SEM methods. As shown in XRD patterns, the intensive peaks, indexed to hexagonal (wurtzite) structure, are observed with no coexistence of other impurity. Also, the XRD patterns of the ZnO-600 before and after photocatalytic reaction (Fig. S7) are similar, indicating the good stability of the ZnO photocatalyst. SEM image of the ZnO-600 after the photocatalytic reaction was depicted in Fig. S8. It can be seen that the morphology of the sample are similar to that of original ZnO-600 catalyst (before the photocatalytic reaction). XRD and SEM tests indicated the ZnO prepared by our solid-phase methods have good stability in structure and morphology.

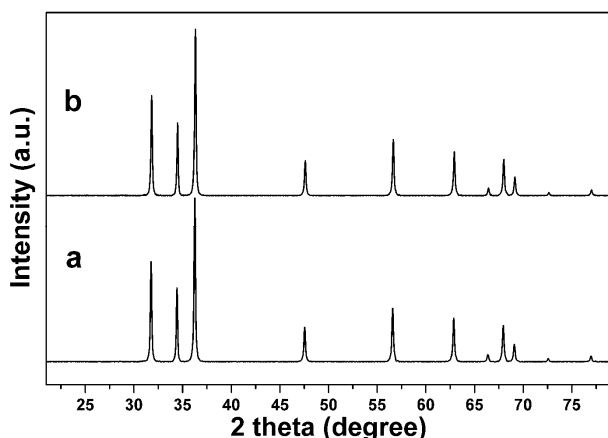


Fig. S7 XRD patterns of the ZnO-600 before (a) and after (b) the photocatalytic reaction.

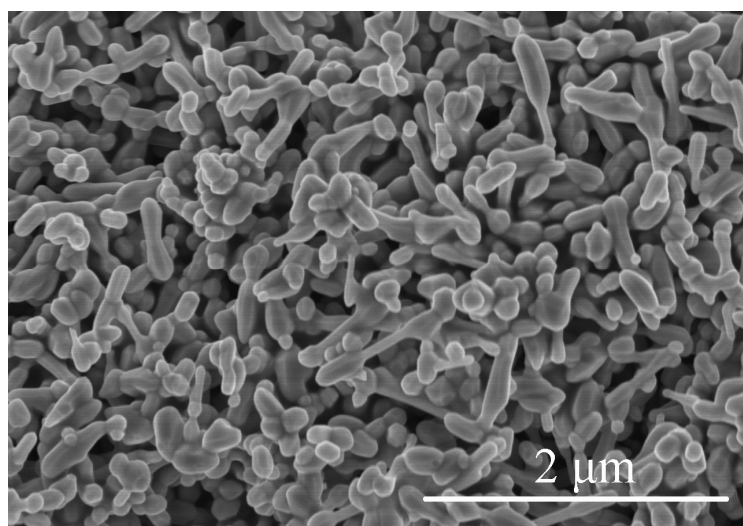


Fig.S8 SEM image of the ZnO-600 after the photocatalytic reaction.

9. XPS analysis

X-ray photoelectron spectroscopy (XPS) is an effective tool for studying the chemical composition of the materials. For semiconductor oxide catalyst, it is very useful for giving the information about oxide species that have direct correlation with the photocatalytic activity of the materials. Fig. S9 show XPS spectra for the Zn2p and O1s core level taken from ZnO-600. It can be seen that the peak position of Zn 2p $_{3/2}$ peak is about 1021.2 eV, indicating that Zn is in the Zn $^{2+}$ valence state. The XPS spectra of O1s from ZnO-600 are composed of three peaks. The peak centered at 529.9 eV is closely associated with the lattice oxygen (O_L) of ZnO, the peak at about

531.3 eV is attributed to the oxygen of surface hydroxyl (O_H), while the peak at 532.7 eV is due to the chemisorbed oxygen (O_a). As has already been proven, surface hydroxyls (O_H) of the photocatalyst play a significant role for a photocatalytic oxidation process. The presence of O_H on the surface cannot only easily capture holes to form active $\cdot OH$ radicals but also can enhance O_2 adsorption to trap electrons and to produce more $\cdot OH$ radicals.

According to the quantitative analysis of XPS data, the corresponding molar percentage of O species from ZnO-600 are carried out, and the results are summarized in Table S1. It can be seen that the molar percentage of O_H in O content is about 26.42%. We believe that such a high percentage of O_H is favorable to improving the activity of the ZnO catalyst.

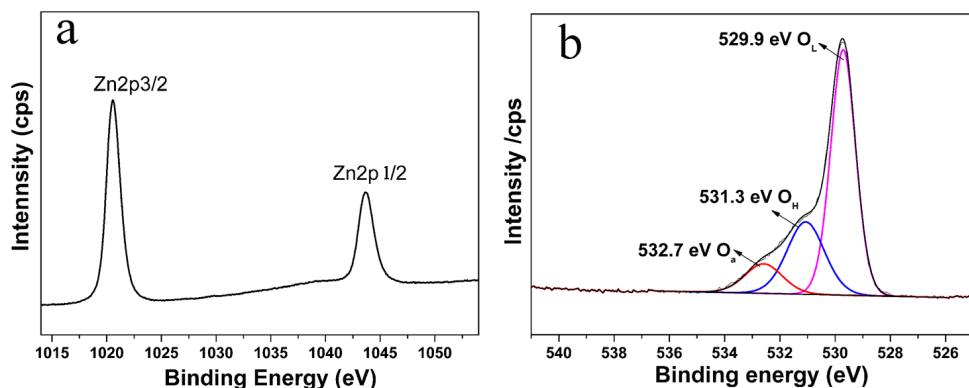


Fig. S9 High-resolution XPS spectra of Zn2p and O1s for ZnO-600.

Table S1 Calculation results for O1s XPS spectra of ZnO-600

| | Lattice oxygen (O_L) | Hydroxy oxygen (O_H) | Adsorbed oxygen (O_a) |
|-----------|--------------------------|--------------------------|---------------------------|
| B.E. (eV) | 529.9 | 531.3 | 532.7 |
| Ri% | 62.39 | 26.42 | 11.19 |

B.E., Binding energy. **Ri**, the percentage of the individual oxygen species in O content calculated from the peak area

10. Catalytic activity for the photodecomposition of RhB and MB dye

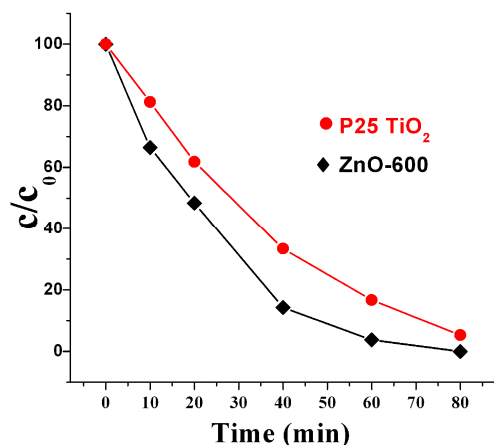


Fig. S10 a) Photodegradation curves of RhB solution by using ZnO-600 and P25 TiO₂ as catalysts under irradiation with UV light;

As shown in Fig.S7, under photo-irradiation, the characteristic absorption of RhB molecular at about 553 nm decreases gradually, and finally almost disappears within 80 min in the presence of ZnO-600 particles. For Degussa P25, the degradation percentage of RhB is about 94% after photo-irradiation of 80 min. The degradation of RhB by Degussa P25 is about 100% for 100 min (Fig. S7). The apparent rate constant for ZnO-600 is 0.055 min⁻¹, which is higher than that of Degussa P25 TiO₂ (0.043 min⁻¹). The result implies that the ZnO-600 have superior photocatalytic ability than Degussa P25 for the photodegradation of RhB dye.

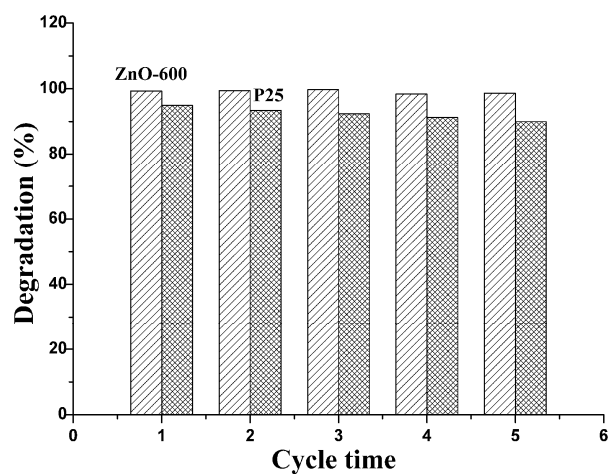


Fig. S11 The reuse activity of ZnO-600 and P25 for the photodegradation of RhB.

In the recycling use for photo-degradation of RhB, the irradiation time for each test is 80 min. As shown in Fig. S8, the photo-degradation efficiency of ZnO-600 has no visible change after five recycles, which is superior to ZnO hierarchical micro/nano-architecture prepared in EDA-water mixed solvent, for which the degradation of the dye decreased from 100% to 95% after three cycles. The results indicated that ZnO-600 photocatalyst has a good reuse performance. As control, the reuse performance of Degussa P25 was also investigated. As shown, the degradation efficiency of RhB is about 90% in five cycles for Degussa P25 catalyst. The decrease in the photocatalytic efficiency of Degussa P25 should be related to the loss of Degussa P25 in reuse cycle due to its excellent dispersion in water, which make it is difficult to totally separate Degussa P25 from the system even with the assistance of high-speed centrifugation.

Table S2: The degradation of Methylene Blue on the P25 TiO₂ and ZnO-600

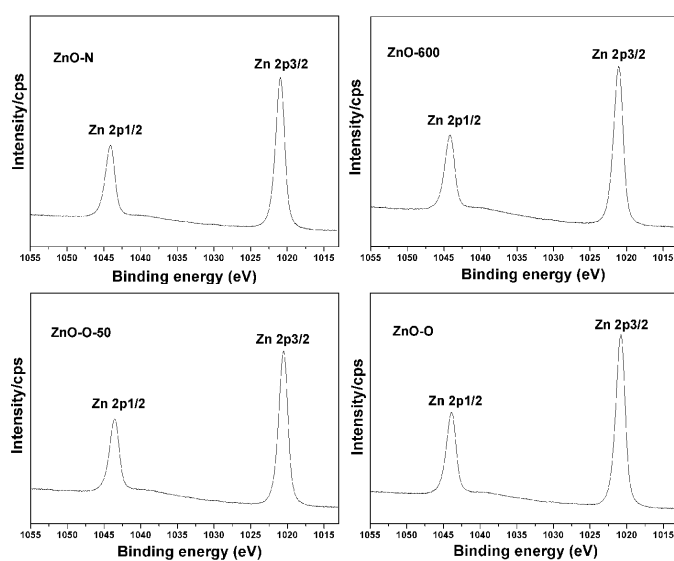
| Catalyst | Pollutant | Time | Degradation (%) |
|----------------------|----------------|---------|-----------------|
| P25 TiO ₂ | Methylene Blue | 100 min | 89% |
| ZnO-600 | Methylene Blue | 100 min | 100% |

11. The effect of the O₂ content in heating atmosphere on the microstructure of the materials

We have investigate primarily the effect of the O₂ content by performing the reaction in the atmosphere at 600°C under the atmosphere of pure O₂, pure N₂, 21%O₂+78%N₂ (Air) and 50%O₂+50%N₂. The samples were denoted as ZnO-O, ZnO-N, ZnO-600 and ZnO-O-50. XRD test indicted that all of the sample are composed of single-phase ZnO with the wurtzite structure.

These samples were analyzed by XPS methods. As shown in **Fig. S12**, the peak of Zn 2p3/2 for all samples is centered about 1021 eV, showing that Zn is in the formal Zn²⁺ valence state. The XPS spectra of O1s for all samples are composed of three peaks. The peak located at ~530 eV is closely associated with the lattice oxygen (O_L)

of ZnO, the peak at \sim 531 eV is attributed to the oxygen of surface hydroxyl (O_H), while the peak position at \sim 533 eV is due to the chemisorbed oxygen (O_a). According to the quantitative analysis of XPS data, the corresponding molar percentage of O species are carried out, and the results are summarized in **Table S3**. We can see that the content of three O species is different for the four samples. Typically, the molar percentage of O_H has a lowest value in ZnO-N sample (19.31%). While for other three samples, the molar percentage of O_H is similar (about 27%). Also, it can be observed that the O_2 content in the synthesis have also effect on the ratio of O_L and Zn. The value is lowest for ZnO-O sample. The XPS analysis indicated that the oxygen content in heating atmosphere have influence on the content of the oxygen species as Referee's said. Besides, we also found that the factor has also effect on other properties of the materials, for examples, the BET surface area. The ZnO-N sample has higher BET surface area (about $9.5\text{ m}^2/\text{g}$), and for ZnO-600, the ZnO-O BET surface area is about $6\text{ m}^2/\text{g}$. ZnO-O-50 and ZnO-O have similar BET specific surface area (about $5\text{ m}^2/\text{g}$). Based on above analysis, we found that the effect of O_2 content in heating atmosphere on the materials is multidimensional. The effect of the parameter on the structure and performance of the materials is under way.



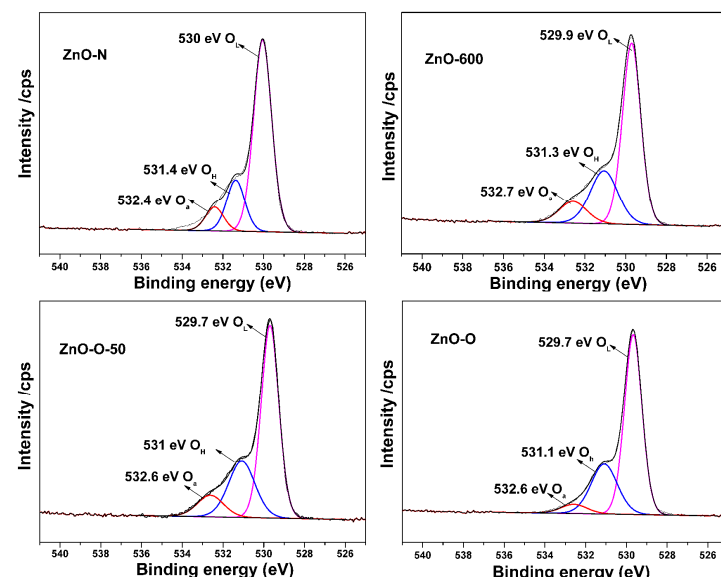


Fig. S12 High-resolution XPS spectra of Zn2p and O1s for ZnO-N, ZnO-600, ZnO-O-50 and ZnO-O.

Table S3 Calculation results for O1s XPS spectra of the different ZnO samples

| Sample | Lattice oxygen (O _L) | | Hydroxy oxygen (O _H) | | Adsorbed oxygen (O _a) | | Molar ratio of O/Zn | Molar ratio of O _L /Zn |
|----------|----------------------------------|-------|----------------------------------|-------|-----------------------------------|-------|---------------------|-----------------------------------|
| | B.E. | Ri% | B.E. | Ri% | B.E. | Ri% | | |
| ZnO-N | 530 | 71.72 | 531.4 | 19.31 | 532.4 | 8.96 | 40.78:37.44 | 0.78 |
| ZnO-600 | 529.9 | 62.39 | 531.3 | 26.42 | 532.7 | 11.19 | 37.63:30.20 | 0.784 |
| ZnO-O-50 | 529.7 | 62.3 | 531 | 27.29 | 532.6 | 10.41 | 35.88:25.93 | 0.7835 |
| ZnO-O | 529.7 | 67.05 | 531.1 | 27.85 | 532.6 | 5.10 | 42.14:42.25 | 0.6687 |

B.E., Binding energy. Ri, the percent of the individual oxygen species calculated from the peak area.